Geothermal Exploration Using Soil CO2 Flux Surveys in Arid Environments

Mark HARVEY[1], Guillermo CHAVEZ[2] and Marcos DELGADO

1University of Connecticut, Storrs, USA

[2]Polaris Energy Nicaragua, San Jacinto Tizate, León, Nicaragua

ABSTRACT

A 20 km^2 soil CO_2 flux survey was conducted at the San Jacinto-Tizate geothermal power project, Nicaragua. Conditions were dry and hot for the entire survey period and the results have negligible interference from biological gas flux. The survey showed a broad area of low CO_2 flux surrounding the central production area, which probably represents the capping formation; the cap prevents gas flux from reaching the surface. An area of relatively high CO_2 flux occurs NNW of the steamfield in close association with i) a magnetic high anomaly, previously interpreted to result from unaltered material, ii) MT resistivity high, and iii) watershed catchment boundaries. The area of high CO_2 flux is hydrologically isolated from the central production area, and may lack a reservoir. This interpretation is supported by a recent reinjection well drilled into the area; early testing showed the well has massive permeability with no pressure connection to the production reservoir. Results suggest CO_2 gas flux surveys are well suited to dry environments (e.g. Atacama Desert, Basin and Range), or in areas with a pronounced dry season (Central America, East Africa). Under these conditions, interference from biological activity is greatly reduced, and CO_2 flux surveys can identify the clay cap as a zone of relatively low CO_2 flux. This is a key goal of geothermal exploration for well targeting.

1. INTRODUCTION

The first exploration wells were drilled at San Jacinto in the early 1990's. A demonstration plant was opened in 2005 then expanded to the current installed capacity (77 MW). Surface thermal features include springs, steaming ground and small fumaroles, which occur at low elevation (relative to surrounding volcanos) near the geothermal production area (El Tizate), and near the village of San Jacinto (**Figure 1**).

CO_2 flux measurements can identify subsurface geothermal activity that may not otherwise be evident. As CO_2 is the major component of typical geothermal gases, and is easily detectable, it is the most appropriate component to focus on.

The CO_2 flux method measures CO_2 emission from ground to atmosphere. In general, CO_2 flux may have one of two sources: deep or shallow (geothermal or biogenic, respectively). Deeply sourced CO_2 may originate from magma at depth beneath the surface (Chiodini et al., 1996). In contrast, biological soil CO_2 flux originates from respiration occurring in shallow soils (plant roots, microbes, and micro-fauna (small animals) (Raich and Schlesinger, 1992).

The process of microbial respiration occurs via the generalized oxidation reaction:

Carbon source (i.e. food) + O2 = CO_2 + H_2O + Energy

The degree of interference to the geothermal CO_2 flux signal caused by this reaction is strongly influenced by the level of biogenic activity in the soil at the time of measurement. This will be controlled by soil moisture, with dry (dehydrated) soils having low to negligible CO_2 flux.

Previously, a 609-point soil CO2 flux survey was undertaken at San Jacinto in the wet season (July) 2011. The purpose was to determine if mapped faults were associated with anomalous CO_2 flux in an area of 20 km2 around El Tizate (Harvey et al., 2011; Figure 1). This survey showed relatively high mean flux (51 g m-2 d-1), which that indicated possible biological signal interference.

Here we provide results from a repeat survey conducted in the dry season (March-April) 2017.

2. METHODOLOGY

Soil gas flux measurements were made using a 100m x 400m grid survey design (**Figure 1**). Flux measurements were made at closer spacing (about 20m) across previously mapped faults to provide higher resolution.

Gas flux measurements were made using a West Systems meter (accumulation chamber method). The accumulation method measures CO_2 flux by placing a 200-mm diameter chamber on the soil surface and pressing it to the soil. CO_2 flowing into the chamber is pumped to an infrared analyser and the CO_2 concentration increase inside the chamber over time is recorded. Concentrate increase is proportional to flux.

CO_2 flux measurements were interpolated by the Sequential Gaussian Simulation (sGs) algorithm within SGeMS (Remy *et al.*, 2009). sGs is a stochastic method that provides more realistic flux maps than kriging (kriging reproduces neither the histogram nor variogram statistics of the original dataset). sGs provides smaller standard deviation than comparable methods when deriving total flow for a survey area (*Cardellini et al.*, 2003), an important advantage for monitoring purposes. CO_2 flux was also interpolated by Kriging (for comparison with 2011 results). A single grid (20x20m) was produced by interpolation algorithms.

Raw data was analysed as follows: (1) computation of experimental variogram; (2) modelling variogram for each data set; and (3) sGs. Datum for all maps is WGS84.

Watershed basins (catchments) for the study area were delineated using SAGA (System for Automated Geoscientific Analyses), GIS software developed for processing digital elevation models (DEM)(*Olaya and Conrad*, 2009); the *Fill Sinks* tool was applied to a 20m and 5m DEM.
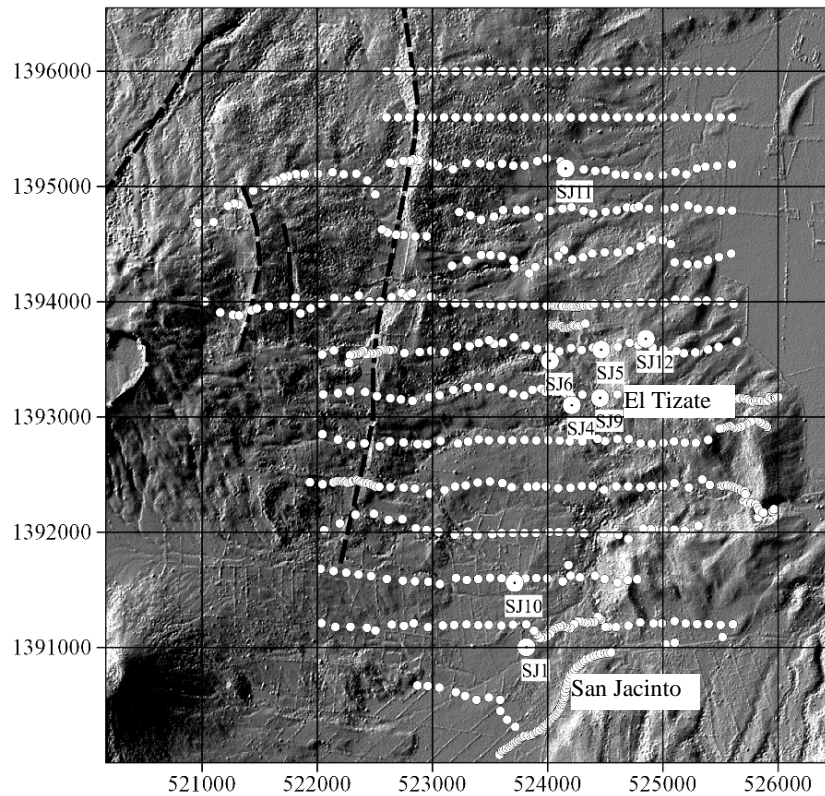
Figure 1: CO_2 flux survey measurement locations (white points) at El Tizate steam field and San Jacinto. Black dash lines show previously interpreted faults. Geothermal wells are labelled.

3. DETERMINATION OF BIOLOGICAL BACKGROUND

To check if soil CO_2 flux measurements were due to biological activity or geothermal sources, a cumulative probability plot was generated (**Figure 4**). Note that inflection or break points in cumulative probability plots can be used to distinguish the presence of multiple populations (Reimann *et al.*, 2005). No such break points are apparent in the plot, suggesting a single population.

The weather during the 2017 survey was dry and hot (mean air temperature 36°C), with almost no rain for the entire survey (February 28 – April 6). The mean CO_2 flux in 2017 (6 g m^{-2} d^{-1}) is much lower than for the 2011 survey (51 g m^{-2} d^{-1})(**Figure 2** - **Figure 3**). It is almost certain the hot, dry conditions dehydrated the soil and practically eliminated biological activity.

The effect of soil moisture was checked by conducting an experiment nearby a sprinkler at San Jacinto. Soil near the sprinkler was wet and vegetated with live grass. Nearby soil (~20m distance) was dry and unvegetated, typical of survey conditions (**Figure 5**B). Six measurements made on each area show the wet soils had CO_2 flux much higher (5-6 times) than nearby dry soils (**Figure 5**B). The dry soil mean (7.5 g m^{-2} d^{-1}) is close to the 2017 mean (5.7 g m^{-2} d^{-1}), whereas the wet soil mean (53 g m^{-2} d^{-1}) is close to the 2011 average (51 g m^{-2} d^{-1}). This result confirms the dry conditions have greatly reduced biological activity in the soil. Accordingly, it is assumed biological CO_2 flux in the 2017 dataset is negligible.
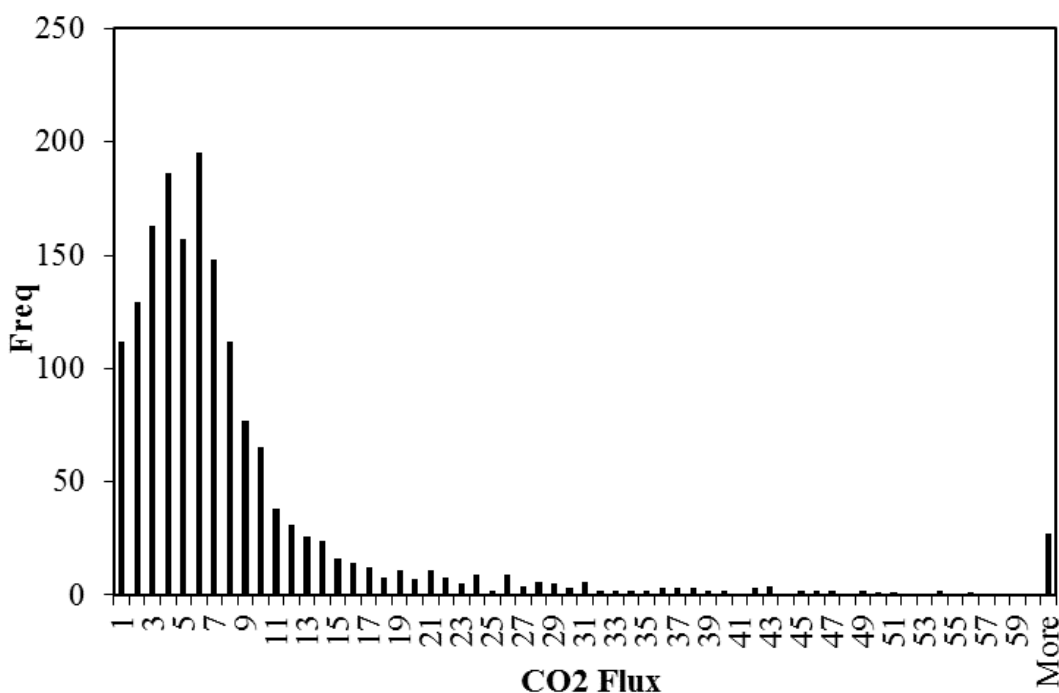

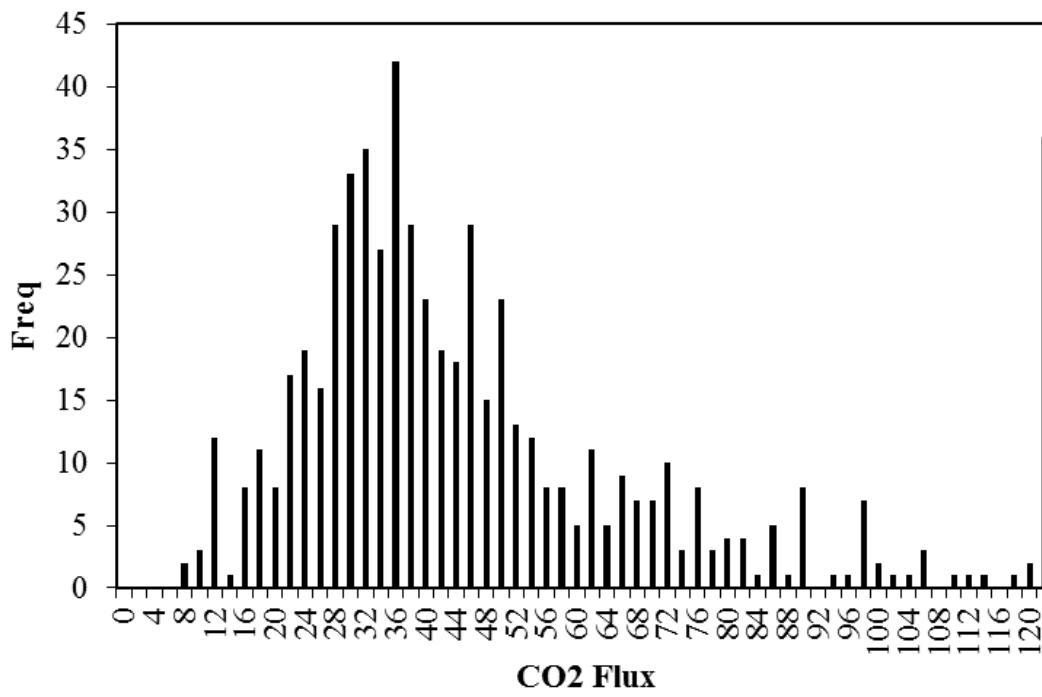**Figure 2:**   **Histogram: 2017 CO_2 flux results (g m^{-2} d^{-1}).**

Figure 3:   Histogram: 2011 CO_2 flux results (g m^{-2} d^{-1}).
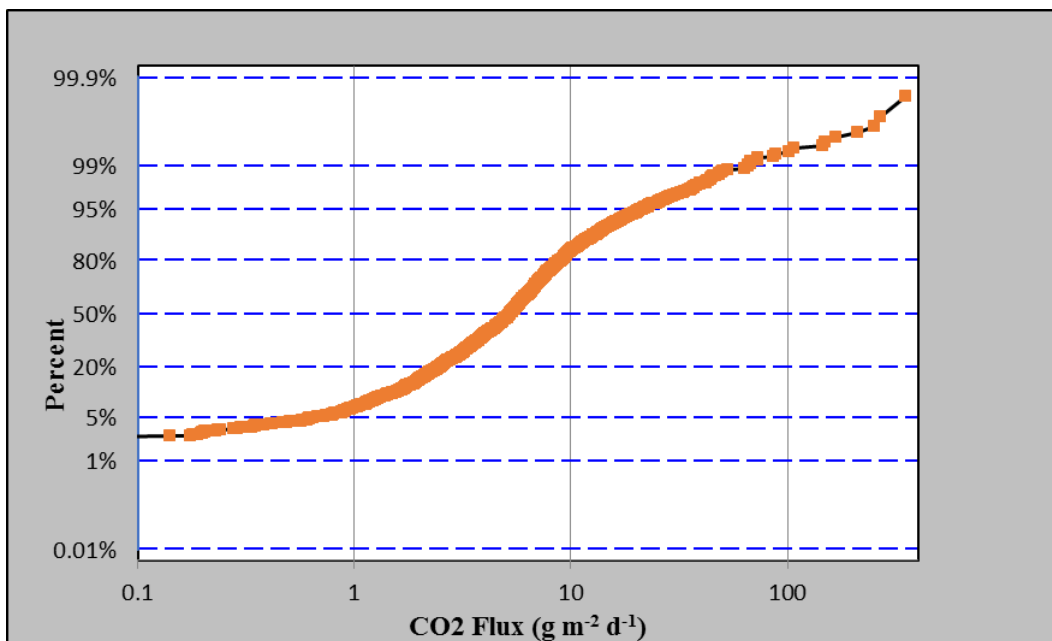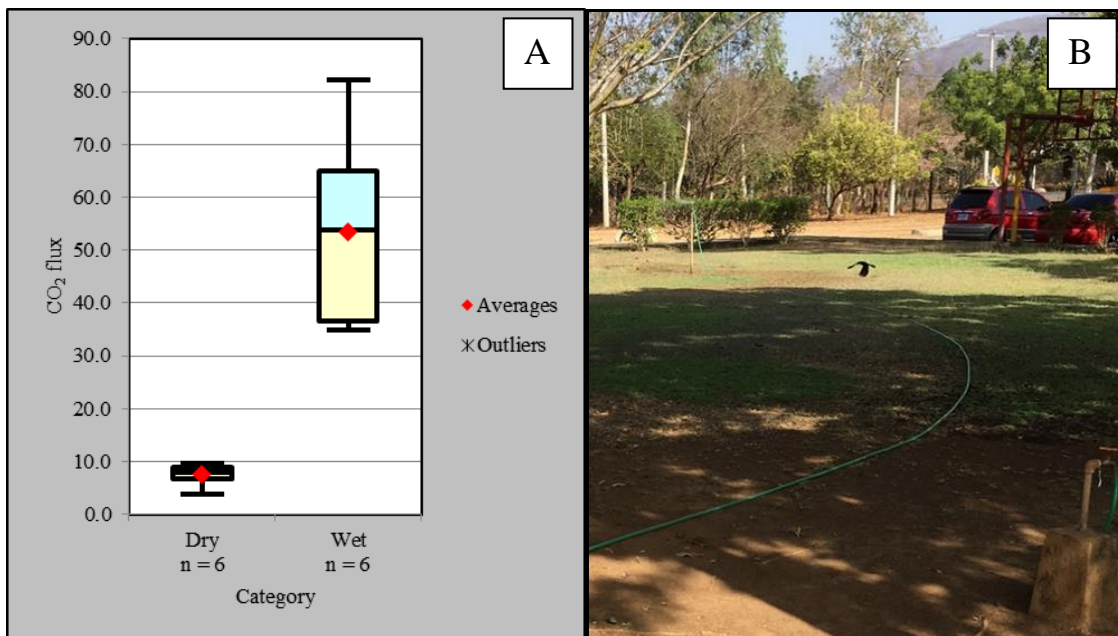

Figure 4:   Cumulative probability plot (all data). Note: the curve is smooth with no obvious breaks.

Figure 5: **(A) Box and whisker plot showing results of experiment comparing CO_2 flux from adjacent soils: moist versus dry. Note i) dry soil average (7.5 g m^{-2} d^{-1}) is close to the 2017 dataset average (5.7 g m^{-2} d^{-1}), and ii) watered soil average (53 g m^{-2} d^{-1}) is close to the 2011 average (51 g m^{-2} d^{-1}). (B) photo of experiment area at offices near San Jacinto village. Note: dry dirt in foreground lacks vegetation. Hose leads to the sprinkler and grass area.**
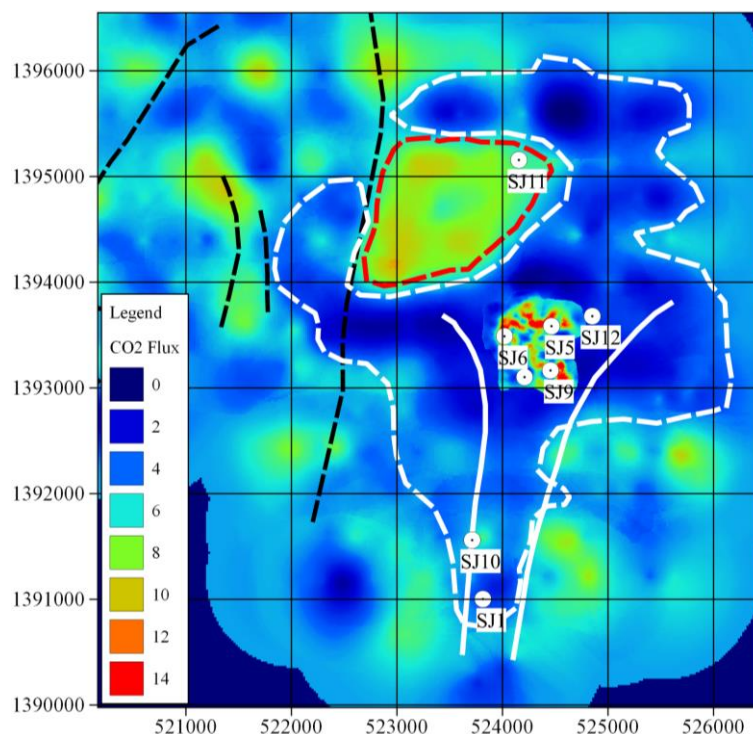
3. RESULTS

609 soil CO_2 flux measurements were collected over 14 field days (28 February - 13 March 2017). A pixel plot shows soil CO_2 flux results (*Figure 6*).

Key observations from *Figure 6*:

A. The production area at El Tizate falls within a low flux zone (LFZ), an area of low CO_2 flux that broadens to the north and narrows to the south (*Figure 6*A). The zone is larger, but of a similar shape to the boundary of the narrow swarm of N-S/NNW-SSE extensional structures, that spreads and shallows northwards (*Figure 6*C), identified by Norini (2016).

B. LFZ is bounded to the NNW by a 1.7 km2 area of high CO_2 flux (*Figure 6*B). This high-flux-zone (HFZ) is bounded to the west by the Los Tablones fault.
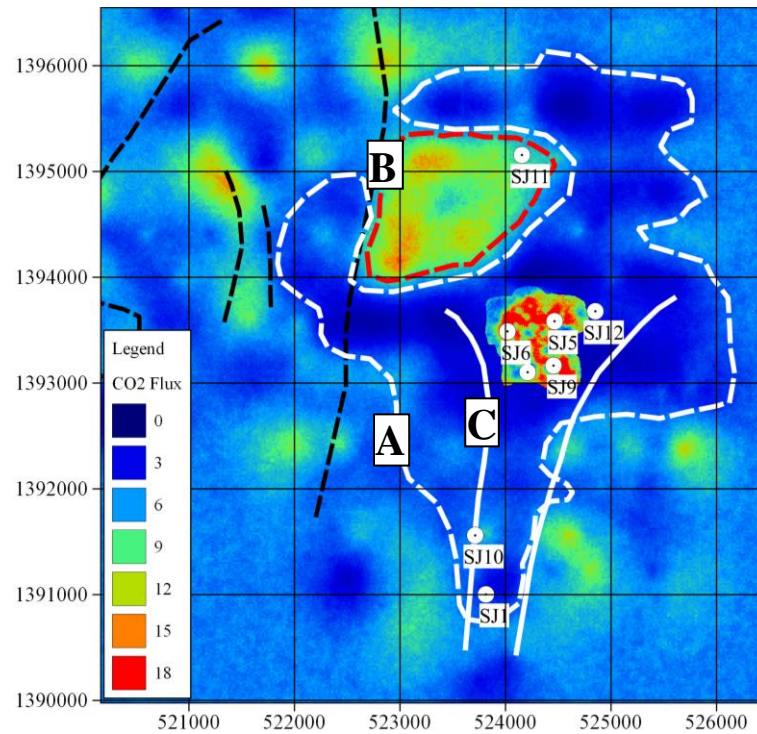
Figure 6: CO_2 flux interpolated by sGs. Note: (A) white dash shows LFZ boundary, (B) HFZ area inside red dash, and (C) structural swarm (Norini, 2016)(solid white). Black dash lines are faults. Geothermal wells are labelled. CO_2 flux units are g m^{-2} d^{-1}. Note: Large area of anomalous CO_2 flux in central production area is associated with thermal ground and based on results from a separate, high-density survey in that area.

Figure 7: CO₂ flux interpolated by Simple Kriging. Note Simple Kriging gives a similar result to sGs result (Figure 6). Black dash lines are faults. Geothermal wells are labelled. CO₂ flux units are g m⁻² d⁻¹.

4. DISCUSSION

Soil Conditions

The weather during the 2017 survey was hot and dry (average ~36°C, February 28 – April 6). The mean CO_2 flux (6 g m⁻² d⁻¹) was much lower than the mean value in 2011 (51 g m⁻² d⁻¹)(Figure 2 - Figure 3). Note, equipment and measurement locations (±5m) were the same for both surveys, so the difference in the mean values results from shallow soil conditions; the previous 2011 survey was undertaken in July when regular rainfall meant that the soil was biologically active.

This conclusion is supported by an experiment compared CO_2 flux in watered to non-watered soils, and showed dry conditions greatly reduce biological activity in the soil. Accordingly, the 2011 CO_2 flux results must now be regarded as heavily contaminated by biological interference. The amount of biological interference, now obvious, was unknown in 2011. The 2017 survey has provided a high-quality data set and the following discussion assumes negligible interference from biological gas flux.

CO₂ flux, structure and watershed basins

The El Tizate central production zone and thermal area is located within a broad low flux zone (LFZ)(7.5 km², average ~4 g m⁻² d⁻¹) that widens to the north and tapers to the south (***Figure 6***A). The LFZ has a similar shape to the narrow swarm of N-S/NNW-SSE extensional structures, which spreads and shallows northwards (***Figure 6***C)(*Norini*, 2016).   Small areas of steam heated ground with intense CO_2 flux degassing that penetrate a much larger clay cap have been noted elsewhere (Werner *et al.*, 2004; Rissmann *et al.*, 2012, Hanson *et al.*, 2014).

It may be the LFZ at El Tizate is associated with the structural swarm, and results from i) rising CO_2 is blocked from reaching the surface by impermeable hydrothermal clays (the clay cap), and/or ii) focussing of reservoir degassing through the El Tizate thermal areas and production wells. The LFZ is bounded to the NNW by the HFZ, a zone (1.7km²) of relatively high CO_2 flux (average ~10 g m⁻² d⁻¹). The area is closely associated with a magnetic high anomaly, previously interpreted to result from unaltered material (i.e. unaffected by hydrothermal activity)(***Figure 8***)(*SKM*, 2011). A previous magnetotelluric survey showed the base of the MT conductor deepens in this area (Figure 9)(SKM, 2011), and preliminary results from a more recent MT survey (2017) suggest a shallow clay cap is absent in this area (Figure 10)(*G. Chavez*, Pers. Comms). In addition, there is no gravity anomaly associated with the HFZ area (SKM, 2011).

Output from watershed modelling shows the southern and western boundaries of the HFZ/magnetic anomaly are closely matched with rainfall catchment boundaries (Figure 11). This compares to the El Tizate thermal area and steamfield that lies within the adjacent southern watershed, which has an extensive catchment to the west (much higher elevation areas to the west). Modelling was repeating using a 5m spatial resolution DSM and gave a similar result (Figure 12).

Implications for the conceptual model of San Jacinto hydrothermal reservoir
The San Jacinto reservoir is situated because of three critical inputs that converge at El Tizate:
- Intrusive that supplies heat
- Structural swarm (permeability)
- Recharge: supply of meteoric water from a large western catchment

Meteoric recharge (rain) at higher elevation in the west drains eastwards. El Tizate is located within a topographic depression where subsurface recharge forms a reservoir; hills immediately to the east of the production area form the eastern catchment boundary, slowing or preventing the subsurface flow from draining to the lowlands further east (Figure 13). The 'captive' recharge is heated and acidified by CO_2 and H_2S rising from beneath. Once acidified, the fluid alters volcanic rocks to clay. An analogous situation exists in the Taupo Volcanic Zone (New Zealand), where hydrothermal systems are also supplied by meteoric recharge (Giggenbach, 1995). Most systems are located along the Waikato River (9 out of 13), which is the primary hydrological drainage channel and topographic low for the Taupo graben (Harvey *et al.*, 2015a; Ratouis and Zarrouk, 2015). The importance of surface topography to system recharge (and the effects on measured CO_2 flux), is discussed by Harvey *et al.* (2015a).

In contrast, the HFZ lies within an adjacent watershed to the north, and lacks i) a large western catchment, and ii) confining hills to the east. Simply put, there may be far less water to engage in water-rock interaction, which would explain the co-occurrence of magnetic high, CO_2 flux high, and shallow resistivity in the HFZ area. This observation leads us to the conclude El Tizate and the HFZ are hydrologically isolated, and to predict that fluids reinjected into the HFZ would do little to support pressure in the El Tizate production reservoir (Harvey Geoscience, 2017).

Validated of this prediction was provided by new re-injection well SJ11-2 (completed June 2017), which penetrates to the HFZ and encountered massive permeability (1100 tons per hour at the bottom of the hole)(***Figure 11***). The well has limited connection to the production reservoir based on the lack of pressure support to the nearby production wells.

Total CO_2 emissions
The mean 2017 CO_2 flux (6 g m^{-2} d^{-1}) multiplied by the survey area (~20 km^2) gives an estimate of natural soil diffuse CO_2 emissions during the survey period: 6 g m^{-2} d^{-1} x 2.0 x 10^7 m^2 = 120 tons CO_2 per day. This is almost twice CO_2 emissions from the power plant: 25,000 tons per year = 69 tons per day.

Comparison with the 2011 survey
It not possible to compare the 2011 and 2017 surveys; this is because in 2011, a threshold between biological/geothermal CO_2 flux populations was assumed (13 g m^{-2} d^{-1}), and "geothermal anomalies" above this threshold were discussed. In 2017, the dataset is assumed to be a single population of geothermal flux (i.e. with negligible biological CO_2 flux). Unsurprisingly, CO_2 flux from 2017 *(*Figure 7*)* bears little resemblance to the 2011 map (***Figure 14***). The explanation is dryer survey conditions in 2017; many "anomalies" reported in 2011 were apparently biological contamination.
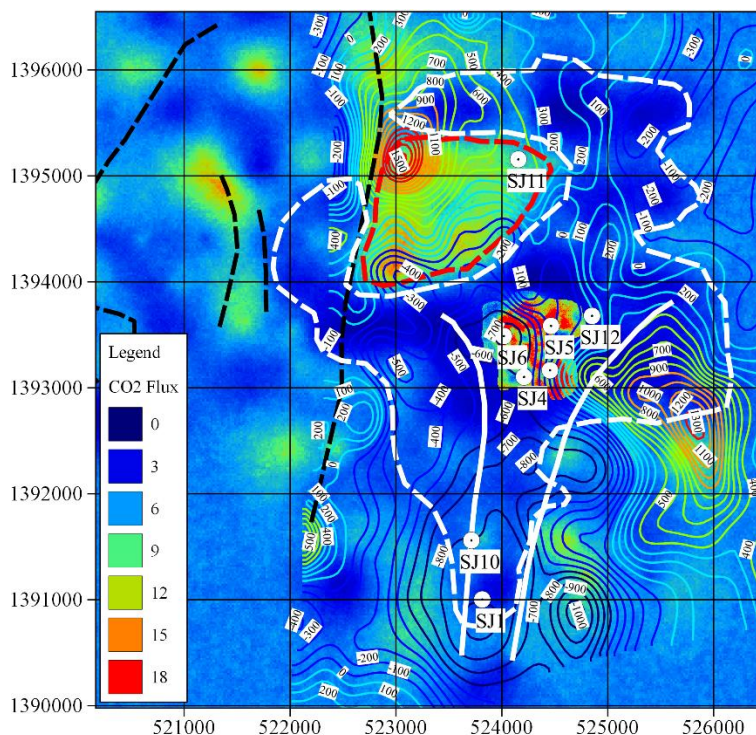
Figure 8. CO₂ Flux results (sGs) plus mag survey contours (nT, reduction to pole). Note: i) HFZ to NNW of steamfield (inside red dash) corresponds to mag high, and ii) LFZ (white dash) corresponds to structural swarm and demagnetized area (SKM, 2011). Black dash lines show Los Tablones and La Joya faults.
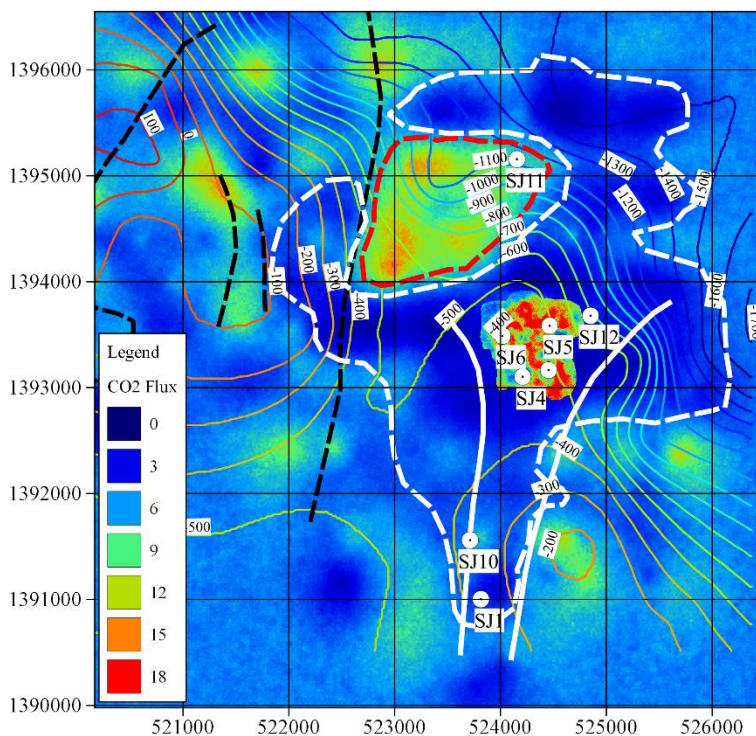
Figure 9. CO₂ flux results (sGs) with MT survey contours (depth to base of conductor)(SKM, 2011). Note: i) HFZ to NNW of steamfield (inside red dash boundary) corresponds to deepening of base of conductor, and ii) LFZ (white dash line) corresponds to structural swarm and MT shallowing of base of conductor. Black dash lines show Los Tablones and La Joya faults.
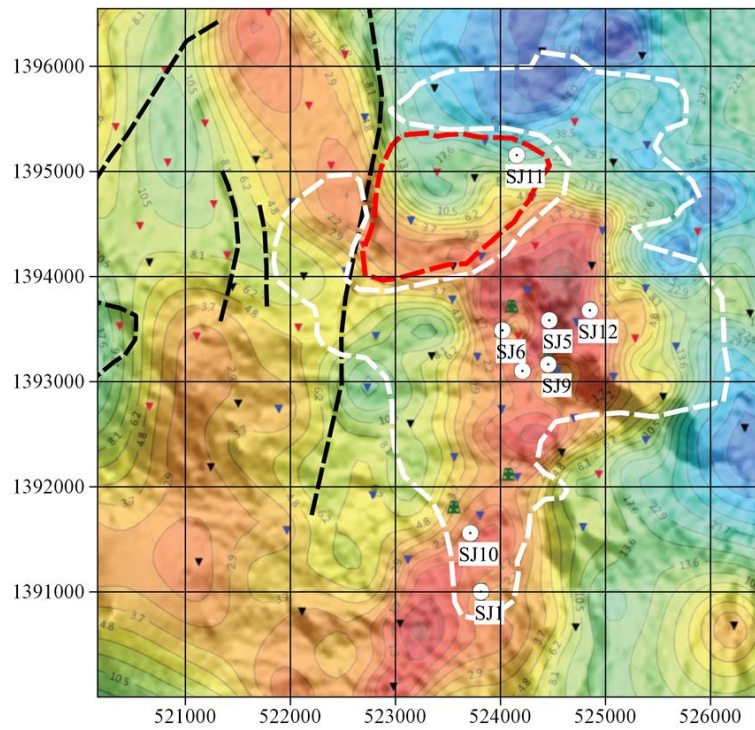
Harvey et al.

Figure 10. Preliminary results from 2017 MT survey: 3D MT inversion – Resistivity at 0m mrsl (ohm.m). Note: HFZ (red dash) corresponds to approx. position of resistivity high at shallow depth. Black dash show Los Tablones and La Joya faults. White dash shows LFZ.
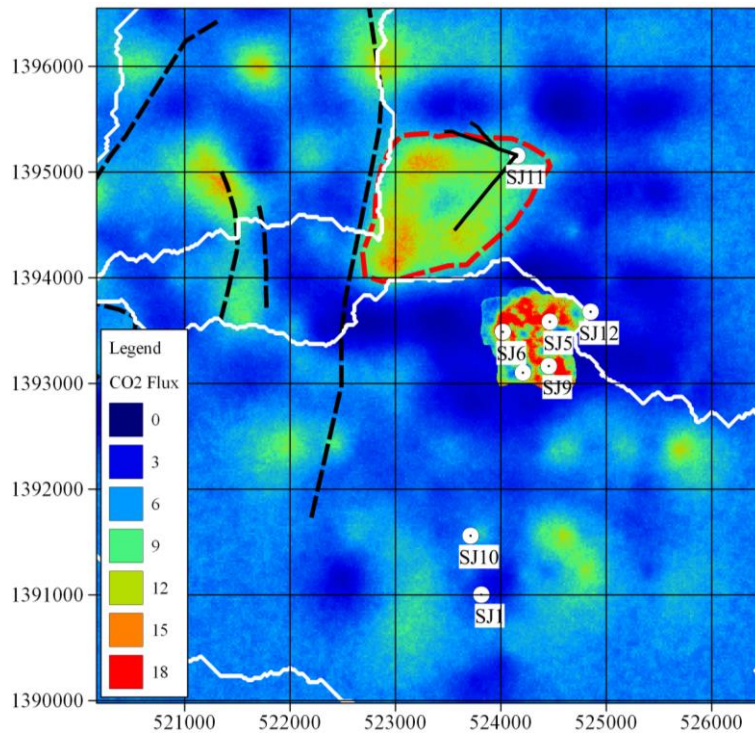

Figure 11. Watershed catchment boundaries (solid white lines, derived from 20m DSM) overlaid on CO_2 flux results (sGs). Note: HFZ (red dash boundary) is bounded to the south and west by watershed boundaries (western watershed boundary is the Los Tablones fault). Black dash show Los Tablones and La Joya faults. Solid black lines show well tracks follow the northern margin of HFZ (SJ11-1) and penetrate HFZ (SJ11-2).
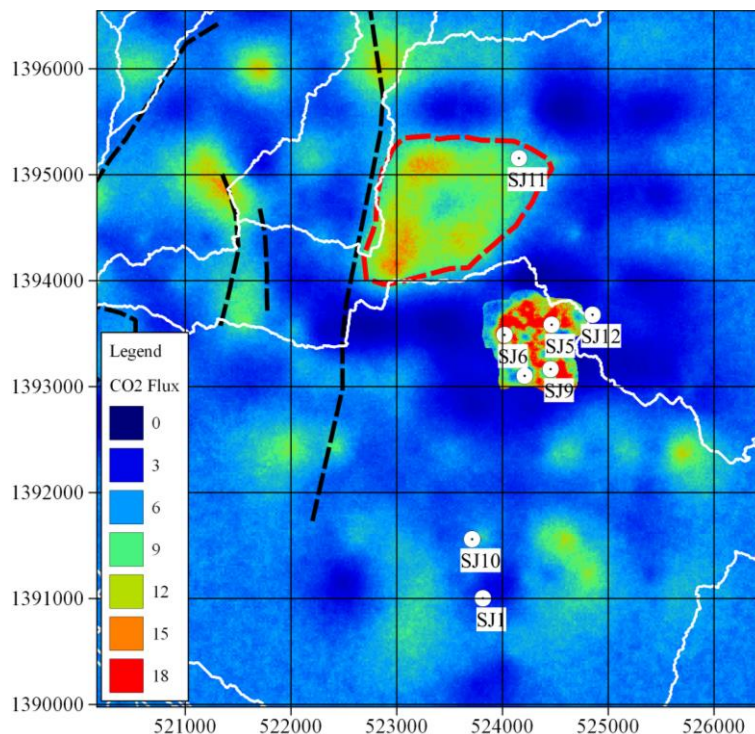
Figure 12. Watershed catchment boundaries (solid white lines, derived from 5m DSM) layered on CO₂ flux results (sGs). Note: the HFZ (inside red dash boundary) is bounded to south and west by watershed boundaries (western watershed boundary is the Los Tablones fault). Black dash lines show Los Tablones and La Joya faults.

Figure 13. View of the El Tizate production area, looking eastwards and down slope into the El Tizate production area valley from the rim of the Los Tablones fault. Recharge flows down toward El Tizate from Los Tablones and the higher elevation catchment to the west. Recharge forms a reservoir at the El Tizate topographic low; note the hill immediately to the east of the production area prevents recharge escaping further east. Recharge is heated and acidified (by CO_2, H_2S), and alters volcanics to clay. White boundary is the LFZ that results from the clay cap. Red boundary encloses HFZ to the north, located on adjacent catchment. Image with vertical exaggeration from Google Earth.
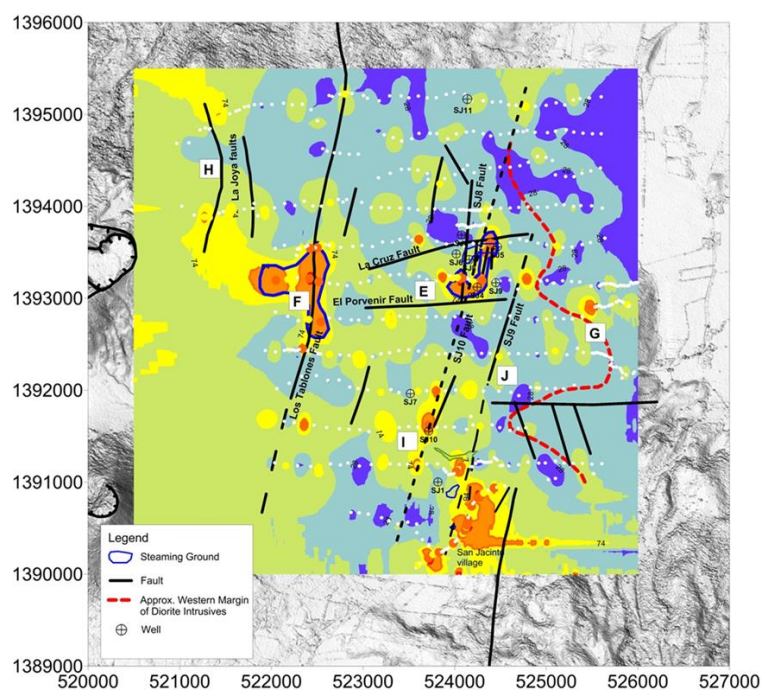
Figure 14. CO$_2$ flux results from 2011, interpolated using Simple Kriging (Harvey et al., 2011).

5.0 CONCLUSIONS

2017 survey conditions were dry and hot for the entire survey period, which provided a high-quality CO$_2$ flux dataset with apparently negligible interference from biogenic gas flux.

A wide area of relatively low CO$_2$ flux (LFZ) surrounds the central production area, which may result from a low permeability capping formation and/or depletion of reservoir CO$_2$ because of production (CO$_2$ is vented by plant). The area partly encircles an area of high CO$_2$ flux (HFZ) to the NNW of the main production area. The HFZ is closely associated with i) a magnetic high anomaly (previously interpreted to result from unaltered material), ii) MT resistivity high, and iii) watershed catchment boundaries. Together with recent drilling results, these observations suggest the HFZ area is hydrologically isolated from the central production area.

Our results suggest CO$_2$ gas flux surveys are particularly well suited to arid environments such as the Basin and Range, Atacama Desert, or other areas with a pronounced dry season (Central America, East Africa). Under these conditions, surveys may be able to identify the clay cap as a zone of relatively low CO$_2$ flux. Identification of the clay cap is a key objective of well targeting and geothermal exploration. In wet climates, or where biological activity is probable, it is recommended that future surveys combine [13]CO$_2$ isotope analysis with CO$_2$ flux measurements to identify biological signal interference (Harvey *et al.*, 2015b).

REFERENCES

Cardellini, C., G. Chiodini, and F. Frondini (2003), Application of stochastic simulation to CO2 flux from soil: Mapping and quantification of gas release, *J. Geophys. Res.: Solid Earth (1978–2012), 108*.

Chiodini, G., F. Frondini, and B. Raco (1996), Diffuse emission of CO$_2$ from the Fossa crater, Vulcano Island (Italy) *Bull. Volcan., 58*, 41-50.

Fridriksson, T., B. R. Kristjánsson, H. Ármannsson, E. Margrétardóttir, S. Ólafsdóttir, and G. Chiodini (2006), CO$_2$ emissions and heat flow through soil, fumaroles, and steam heated mud pools at the Reykjanes geothermal area, SW Iceland, *Appl. Geochem., 21*, 1551-1569.

Giggenbach, W. F. (1995), Variations in the chemical and isotopic composition of fluids discharged from the Taupo Volcanic Zone, New Zealand, *J. Volcanol. Geotherm. Res., 68*, 89-116.

Hanson, M.C., Oze, C., and Horton, T.W. (2014), Identifying blind geothermal systems with soil CO$_2$ surveys. *Applied Geochemistry, 50,* 106–114.

Harvey, M. C., P. J. White, K. M. MacKenzie, and B. G. Lovelock (2011), Results from a soil CO$_2$ flux and shallow temperature survey at the San Jacinto-Tizate geothermal power project, Nicaragua, *New Zealand Geothermal Workshop Proceedings*.

Harvey, M. C., Rowland, J. V., Chiodini, G., Rissmann, C. F., Bloomberg, S., Hernández, P. A., Mazot, A., Viveiros, F., and Werner, C. (2015a). Heat flux from magmatic hydrothermal systems related to availability of fluid recharge. *Journal of Volcanology and Geothermal Research*, 302, 225-236.

Harvey, M. C., Zygadlo, M., and Dwivedi, A. (2015b), Use of isotopic analysis to distinguish between biological and geothermal soil CO_2 flux at Tauhara and Te Mihi geothermal areas. In *Proceedings 37rd New Zealand Geothermal Workshop*.

Harvey Geoscience (2017), Soil CO_2 Flux and Shallow Temperature Survey San Jacinto, March-April 2017. Client Report.

Norini (2016), Volcanotectonic study of the San Jacinto-Tizate concession and implications for the geothermal exploration. Client report.

Olaya, V., & Conrad, O. (2009). Geomorphometry in SAGA. *Developments in Soil Science*, *33*, 293-308.

Raich, J. W., and Schlesinger, W. H. (1992). The global carbon dioxide flux in soil respiration and its relationship to vegetation and climate. *Tellus B*, 44, 81-99.

Ratouis, T. M., & Zarrouk, S. J. (2016), Factors controlling large-scale hydrodynamic convection in the Taupo Volcanic Zone (TVZ), New Zealand. *Geothermics*, *59*, 236-251.

Reimann, C., Filzmoserb, P., & Garrett, R.G. (2005), Background and threshold: critical comparison of methods of determination. Science of the Total Environment, Vol. 346, pp. 1-16.

Remy, N., Boucher, A., & Wu, J. (2009), *Applied geostatistics with SGeMS: A user's guide*. Cambridge University Press.

Rissmann, C., B. Christenson, C. Werner, M. Leybourne, J. Cole, and D. Gravley (2012), Surface heat flow and CO_2 emissions within the Ohaaki hydrothermal field, Taupo Volcanic Zone, New Zealand, *Appl. Geochem., 27*, 223-239.

SKM (2011), San Jacinto - Interpretation of 2011 Gravity and magnetic surveys. Client report.

SKM (2012), Well SJ11-1 Geology and Petrology Report. Client Report.

Werner, C., Hochstein, M. P., & Bromley, C. (2004). CO2 fluxes of steaming ground at Karapiti (Wairakei, NZ). In *The 26th New Zealand Geothermal Workshop/GEO3, Taupo, New Zealand*.